International Journal of Hydrogen Energy 136 (2025) 102–114

Contents lists available at ScienceDirect

International Journal of Hydrogen Energy

journal homepage: www.elsevier.com/locate/he

Dynamic evolution of CO_2 hydrogenation to methanol over Cu catalysts based on ReaxFF MD simulations

Meirong Dong [a,b,*], Zehua Huang [a,b], Junchang Xiong [a,b], Hongchuan Liu [a,b], Youcai Liang [a,b], Jidong Lu [a,b]

[a] School of Electric Power Engineering, South China University of Technology, Guangzhou, Guangdong, 510640, China
[b] Guangdong Province Engineering Research Center of High Efficient and Low Pollution Energy Conversion, Guangzhou, Guangdong, 510640, China

ARTICLE INFO

Handling Editor: Jinlong Gong

Keywords:
Methanol synthesis
Cu surfaces
ReaxFF MD
Reaction pathways
Kinetic effects

ABSTRACT

It is essential to identify key intermediates for elucidating the reaction mechanism by studying the dynamic evolution of the reaction process. In the synthesis of methanol by CO_2 hydrogenation, the formation of by-products CO and H_2O affects the selective generation of methanol. In this work, reactive force field molecular dynamics (ReaxFF MD) simulations were proposed to simulate the CO_2 hydrogenation reaction on Cu surface. The CO_2/H_2, $CO_2/CO/H_2$ and $CO_2/H_2O/H_2$ systems were analyzed sequentially in order to explore the dynamic properties of the key intermediate product generation and to elucidate the detailed reaction pathways and their kinetic effects. The results showed that in the CO_2/H_2 system, there are three different pathways for the methanol production, while two main pathways were found for CO hydrogenation. The synergistic effect between CO_2 and CO hydrogenation was demonstrated in the CO_2/CO co-hydrogenation to methanol, and the introduction of CO further improved the methanol selectivity. However, in the CO/H_2 system, excessive CO adsorption leads to severe C deposition, catalyst deactivation, and reduced methanol yield. Conversely, the incorporation of H_2O into the CO_2/H_2 system was shown to inhibit the C deposition on the Cu catalyst, maintain the catalytic activity, and enhance the methanol selectivity by introducing the methoxy hydrolysis pathway ($CH_3O + H_2O \rightarrow CH_3OH + HO$). It is worth noting that the simulations revealed previously unrecognized CH pathways ($CO_2 \rightarrow CH \rightarrow CH \rightarrow CHO \rightarrow CH_2O \rightarrow CH_3O \rightarrow CH_3OH$) and methoxy hydrolysis pathways. The proposed route to synthesize methanol over Cu catalysts not only provides novel insights into methanol synthesis, but also provides the necessary theoretical support for understanding the reaction mechanism of CO_2 hydrogenation to methanol.

1. Introduction

The rising concentration of CO_2 in the atmosphere, which has increased from about 280 ppm in the pre-industrial era to about 422 ppm in 2024 [1], poses a serious challenge to global climate stability. To mitigate the adverse effects of greenhouse gas emissions, Carbon Capture, Utilization, and Storage (CCUS) has been developed imperatively. CO_2 exhibits high thermodynamic stability and chemical inertness. However, when coupled with hydrogen in the presence of catalysts, it can be activated and converted into valuable chemicals or fuels, including methanol, carbon monoxide, methane, dimethyl ether, and multi-carbon compounds [2]. The hydrogen required for this process can be sourced from biomass or via water electrolysis powered by renewable energy sources such as solar, tidal, and wind energy, which is called green hydrogen [3]. Although hydrogen is the least volumetrically energy dense energy source with good prospects for development and application, it also suffers from high transportation costs and difficulties in storage and transportation [4].

Methanol, as a liquid with well-established infrastructure, has been identified as a potentially efficient medium for the storage of renewable energy sources and for producing hydrogen via reforming technology, making it an ideal carrier for hydrogen energy [5,6]. The catalytic preparation of methanol by the hydrogenation of CO_2 with H_2 is conducted at pressures of 15–50 bar and temperatures of 200–350 °C. The main reaction can be expressed as [7]:

$$CO_2+3H_2 \rightarrow CH_3OH + H_2O,\ \triangle H_{298K} = -49.4\ \text{kJ/mol}\ (1)$$

Alternatively, it can be synthesized by indirect hydrogenation of CO_2, which is first converted to CO by reverse water-gas shift (RWGS).

* Corresponding author. School of Electric Power Engineering, South China University of Technology, Guangzhou, Guangdong, 510640, China.
E-mail address: epdongmr@scut.edu.cn (M. Dong).

https://doi.org/10.1016/j.ijhydene.2025.05.049
Received 24 January 2025; Received in revised form 2 May 2025; Accepted 5 May 2025
Available online 9 May 2025

The RWGS reaction is as follows:

$$CO_2+H_2 \rightarrow CO + H_2O,\ \triangle H_{298K} = 41.2\ kJ/mol \quad (2)$$

Then methanol is formed through CO hydrogenation reaction:

$$CO+2H_2 \rightarrow CH_3OH,\ \triangle H_{298K} = -90.6\ kJ/mol \quad (3)$$

Cu-based catalysts have become the most commonly used catalysts due to their low cost, high stability, and excellent performance in CO_2 conversion and CH_3OH selectivity [8]. Extensive experimental and theoretical studies have been conducted on the reaction pathways of Cu-based catalysts to enhance the efficiency of CO_2 hydrogenation to methanol [7,9–12]. Based on the surface structural properties of Cu-based catalysts, the regulatory effects of supports and additives, and the influence of reaction conditions, three primary mechanisms for CO_2 hydrogenation have been identified: the formate (HCOO) pathway, the *trans*-COOH* pathway, and the RWGS + CO-Hydro pathway [13]. In the formate pathway [14–17], CO_2 has first combined with atomic hydrogen to form HCOO*, which has then been further hydrogenated to form HCOOH*, followed by continued hydrogenation to form H_2COOH*, which has been cleaved to H_2CO* and *OH, with H_2CO subsequently hydrogenated to form CH_3OH. This conclusion is primarily based on experimental observations that show HCOO as the most abundant surface intermediate in the CO_2 hydrogenation process. Except for the formate pathway, DFT calculations suggest the existence of an alternative *trans*-COOH pathway [18,19]. In this pathway, the initial hydrogen atom binds preferentially to the oxygen atom of the CO_2 molecule to form a COOH intermediate rather than attaching to the carbon, followed by the formation of dihydroxycarbene (COHOH*) as the reactive species, which is eventually converted to CH_3OH. On the other hand, methanol formation via the RWGS pathway begins with the conversion of CO_2 to CO*, which is subsequently hydrogenated to methanol through the formation of HCO*. This pathway may also involve the formation of COOH*, which are further converted to CO*. COOH* intermediates are generated by the reaction of CO_2 with hydrogen atoms supplied by H_2O. Consequently, this pathway is designated as a H_2O-mediated mechanism. However, most of the existing studies focus mainly on static reaction paths with limited consideration of the real-time dynamic evolution of the reaction.

The dynamic evolution of the reaction process is of great research value in revealing the reaction mechanism of CO_2 hydrogenation to methanol. It can reveal new intermediates and reaction steps that emerge during the process [20]. Reactive force field molecular dynamic (ReaxFF MD) simulations are particularly suitable for studying large-scale chemical reaction systems involving complex reactions [21–23]. This method has been effectively applied to explore reaction mechanisms in carbonaceous materials, such as biomass [24], coal precursors [25], biofuels [26], and petroleum derivatives [27]. Yao et al. used ReaxFF to simulate the pyrolytic polypropylene process of iron under microwave irradiation conditions [28]. In addition, the method has been used to study the early carburization behavior on iron oxides [29], to combine DFT and ReaxFF to study the syngas methanation reaction over Ni-based catalysts [30], and to investigate the reaction kinetics of CO_2 hydrogenation over Fe catalysts [31]. However, due to the inherent limitations of the force field, most studies have focused on transition-metal catalysts (e.g., Fe [31,32], Cu [21], and Ni [30]), particularly in gas-solid catalyzed reactions, where their behavior is more typical and has become the main research focus.

It is worth noting the presence of H_2O and CO as by-products during the hydrogenation of CO_2 to methanol. Wang et al. [33] conducted in-situ DRIFT experiments under both hydrous and anhydrous atmospheres, demonstrating that H_2O participates in methanol formation through the hydrolysis of methoxy groups, thereby promoting methanol production. However, Stangeland et al. [34] argued that H_2O, as a by-product of methanol synthesis from CO_2, competes for adsorption on the active sites of the catalyst, leading to catalyst deactivation. There is also currently some controversy regarding the presence of CO and its effect on the reaction. Nielsen et al. [35] confirmed that CO exhibits pure inhibition of Cu catalysts at low conversions with almost negligible product generation. Nevertheless, Vu et al. [36] showed that CO hydrogenation to methanol is thermodynamically more favorable compared to CO_2 and avoids the inhibition of methanogenesis by H_2O by-products at low temperatures. Liu et al. [37] found that Fe_1Zn_1-imp catalysts with moderate ratios of Fe_5C_2 to Fe_3O_4 promoted both the RWGS and CO hydrogenation reactions, thereby enhancing the overall CO_2 hydrogenation. Grabow et al. [11,38] found that high H_2 pressure not only facilitates the hydrogenation of CO_2, but also generated CH_3OH by promoting the co-hydrogenation of CO and CO_2. In a word, the impact of these by-products on the reaction pathway remains unclear, necessitating further investigation into the roles and effects of CO_2/CO and CO_2/H_2O under coexistence conditions.

The purpose of this study is to gain insight into the reaction mechanism of CO_2 hydrogenation to methanol under different reaction conditions. To achieve this, the dynamic process of CO_2/CO and syngas hydrogenation to methanol on the Cu surface with different hydrogen-to-carbon ratios was simulated using ReaxFF MD simulations. The generation and disappearance of species in the reaction were analyzed at the molecular level, focusing on key intermediates such as CO, COHO, OH, HCO, CH, CH_2O and CH_3O and their reaction pathways. The reaction rates and activation energies of each reaction step were subsequently revealed through further reaction kinetic analysis. In addition, the effects of H_2O on the pathways and kinetics of CO_2 hydrogenation were investigated, which extended the existing reaction pathways and provided new insights for understanding the reaction mechanism and optimizing the catalytic performance.

2. Computational methods and details

2.1. ReaxFF MD simulations

Molecular dynamics simulations were carried out under periodic boundary conditions (PBC) using the ReaxFF module of the LAMMPS package [39,40]. ReaxFF is an empirical force field that employs the bond-length/bond-order and bond-order/bond-energy relationships to achieve smooth transitions between bonded and nonbonded systems [41,42]. During an MD run, the bond orders are updated at each iteration, ensuring that the potential energy of the system accurately reflects the current bonding configurations. This dynamic adjustment allows for a realistic representation of chemical processes, enabling ReaxFF to capture the complexities of reaction mechanisms in a variety of systems. The primary advantage of ReaxFF over earlier reactive force fields lies in its incorporation of non-bonded interactions, such as van der Waals forces and Coulombic terms, which are calculated between every pair of atoms in the system. The potential energy of the system in ReaxFF is expressed as follows:

$$E_{system} = E_{bond} + E_{over} + E_{under} + E_{val} + E_{pen} + E_{tors} + E_{conj} + E_{vdWaals} + E_{Coulmob} \quad (4)$$

where E_{bond} is bond energy, E_{over} and E_{under} represent the over coordination penalty energy and under coordination penalty energy. E_{val}, E_{pen}, E_{tors}, E_{conj}, $E_{vdWaals}$ and $E_{Coulmob}$ represent valence angle energy, additional penalty energy, torsion angle energy, energy contributed by conjugation effects, van der Waals energy and Coulomb energy, respectively. The ReaxFF force field parameters employed in this study are specifically tailored for the Cu/C/H/O system [21]. It has been verified that for the methoxy (-CH_3O) reaction on the Cu surface, about 30 % of the free radicals are converted to stable gas-phase molecules, including methanol (CH_3OH) and formaldehyde (CH_2O).

The simulations were performed using a velocity-Verlet integrator with a time step of 1 fs. Initially, the system was equilibrated at 10 K under the NPT ensemble for 3000 steps, followed by a temperature ramp

to the target values (500 K, 600 K, 700 K, 800 K, 900 K) over 10 ps using the NVT ensemble, controlled by a Nose-Hoover thermostat [43] with a damping constant of 10 fs. Finally, the system was maintained at the set temperatures in the NVT ensemble for 1000 ps until thermodynamic equilibrium was reached. The temperature in the simulation is usually slightly higher than the industrial production temperature, on the one hand due to the difference between the established physical model and the actual process, on the other hand in order to speed up the reaction and shorten the simulation time of the reaction. This approach has been demonstrated to be a reasonable methodology for the detection of reaction intermediates that are challenging to identify under typical experimental conditions [27,44–46].

2.2. Structural optimisation and simulation models

In this work, the stabilized structure of optimized Cu was selected as the protocell, and a 21.69 Å × 21.69 Å × 50.00 Å periodic box was chosen for ReaxFF simulations in the calculations, as shown in Fig. 1. The bottom layer of the simulation system is a Cu(111) surface with a three-layer structure, chosen to strike a balance between computational efficiency and simulation accuracy. The top layer, on the other hand, consists of various ratios of CO_2, H_2, CO, and H_2O. Each model was designed to study the dynamic evolution of the methanol synthesis reaction process, allowing us to investigate real-time reaction pathways under different reaction conditions.

It is important to note that industrial processes frequently function under conditions that are hydrogen-rich [47], and hydrogen-to-carbon ratios (R = 4–10) were selected in this study to simulate a high hydrogen environment. It cannot only facilitate the catalytic reaction but also help reduce the MD simulation time. Six different reaction systems (CO_2:H_2 = 100:1000, CO_2:H_2 = 200:1000, CO:H_2 = 100:1000, CO_2:CO:H_2 = 50:50:1000, CO_2:CO:H_2 = 50:150:1000, and CO_2:H_2:H_2O = 100:940:60) were constructed to represent the different phases of the actual process and the corresponding intermediates (Table 1). The extraction of chemical kinetic mechanisms was achieved through the utilization of a combination of the Chemical Trajectory Analyzer (ChemTraYzer, version 2.1) [48] and the Reaction Network Generator (ReacNetGenerator) [49].

Table 1
Input conditions for different analogue systems.

Parameters system	H_2[a]	CO_2	CO	H_2O	φ[b]	R[c]
CO_2/H_2	1000	100	0	0	10:1	9.0
CO_2/H_2	1000	200	0	0	5:1	4.0
CO/H_2	1000	0	100	0	10:1	10.0
$CO_2/CO/H_2$	1000	50	50	0	20:1:1	9.5
$CO_2/CO/H_2$	1000	150	50	0	20:3:1	4.75
$CO_2/H_2/H_2O$	940	100	0	60	9.4:1	8.4

[a] Quantity of H_2 molecules in the system.
[b] φ represents H_2/CO_x ratio.
[c] R represents hydrogen-carbon ratio, defined as $\frac{H_2 - CO_2}{CO_2 + CO}$ [50].

3. Results and discussion

3.1. CO_2 hydrogenation process and reaction pathways

To evaluate the effect of varying hydrogen-carbon ratio on the reaction behavior, the catalytic process of CO_2 hydrogenation on the Cu surface was first simulated by constructing two systems with hydrogen-to-carbon ratios of R = 9 (CO_2:H_2 = 100:1000) and R = 4 (CO_2:H_2 = 200:1000). The various stages of the process and the corresponding intermediate products were subsequently analyzed. Additionally, to investigate the impact of temperature on the catalytic process, the reaction process was systematically investigated at different temperatures from 500 K to 900 K to obtain the key effects of temperature on product distribution, reaction rate, and reaction mechanism.

Fig. 2a–b shows the evolution of H_2 consumption and CO production, respectively, over time for different hydrogen-carbon ratios in the temperature range of 500–900 K. The solid line shows the hydrogen-carbon ratio R = 9 and the dashed line shows the variation at R = 4. It can be found that the consumption of H_2 is lower at the hydrogen-carbon ratio R = 9, whereas the consumption of H_2 at R = 4 is about twice as much as that at R = 9. In the initial stage of the reaction, the CO generation is rapid. For R = 4, due to the higher feed of CO_2, a large amount of CO is generated rapidly at the beginning of the reaction. The higher the temperature, the faster the reduction of CO, and the number of CO molecules tends to stabilize after 500 ps, remaining at a low level. In contrast, at R = 9, less CO is generated and the number of CO molecules decreases to near zero as the reaction progresses. This suggests

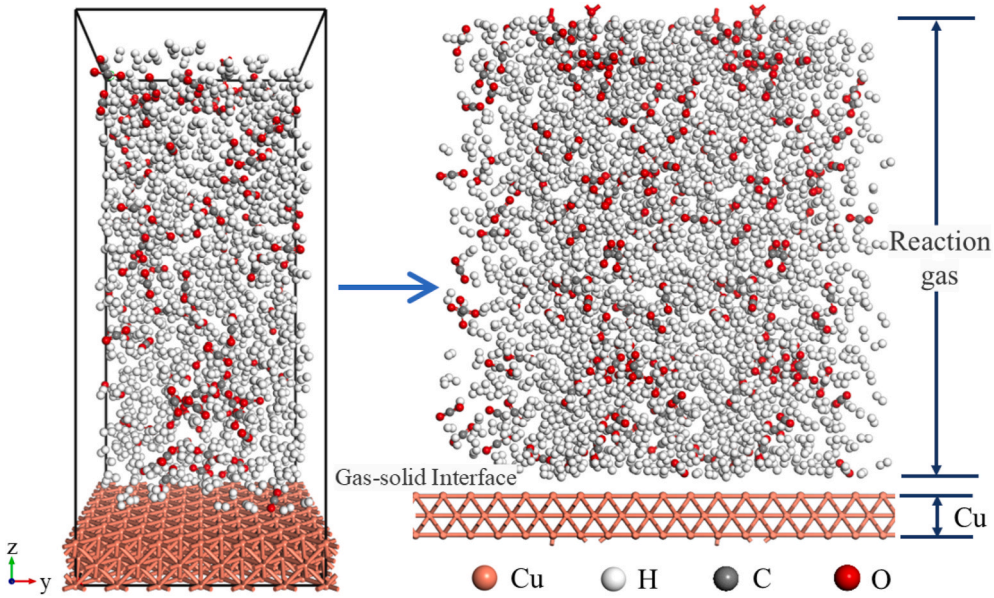

Fig. 1. Initial model of Cu surface reaction with CO_2 and H_2.

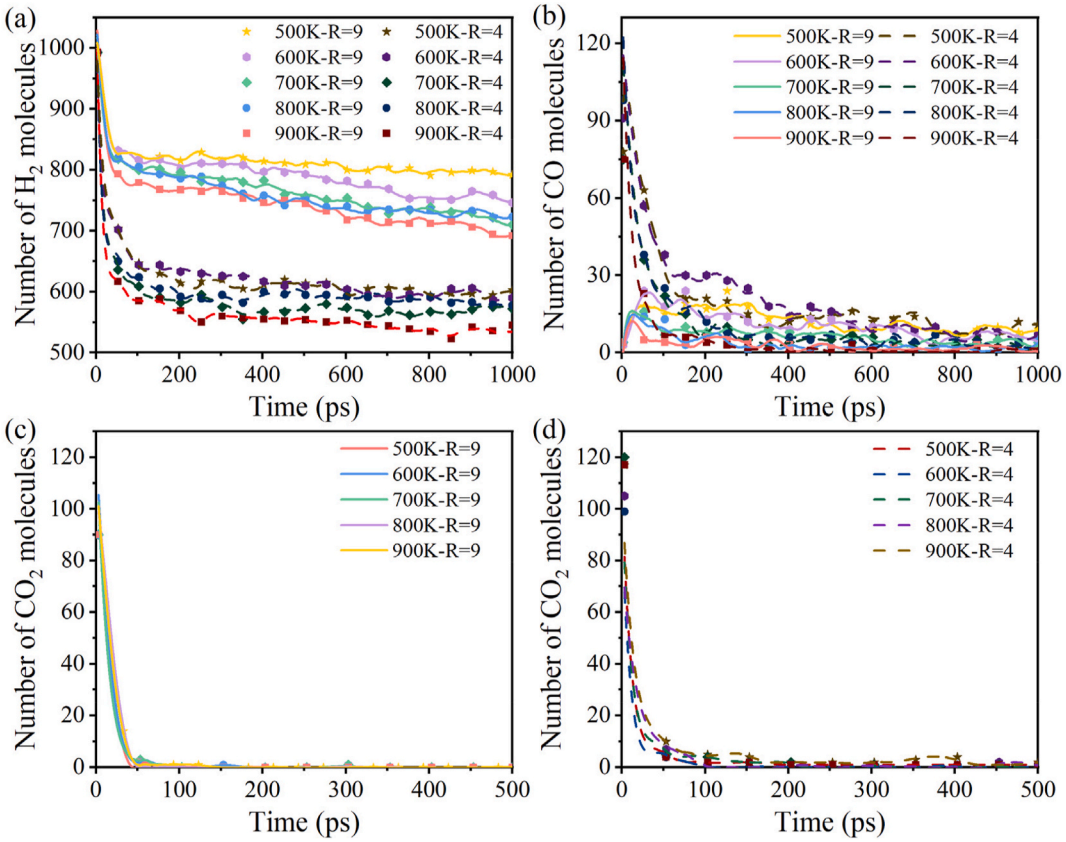

Fig. 2. Temporal evolution of the number of key species during the reaction on the Cu surface. for input gas compositions R = 9 (CO_2:H_2 = 100:1000) and R = 4 (CO_2:H_2 = 200:1000): (a) H_2 consumption (b) CO production (c) CO_2 consumption for R = 9 (d) CO_2 consumption for R = 4.

that in systems with higher hydrogen concentrations (R = 9), CO is more efficiently consumed, and higher temperatures promote the reduction of CO, making them more favorable for the reaction. Fig. 2c and d illustrate the consumption of CO_2 at different hydrogen-carbon ratios. The results show that CO_2 is almost completely consumed within 50 ps at R = 9, whereas at R = 4, CO_2 is nearly completely consumed at about 100 ps. This can be attributed to the higher hydrogen availability in the R = 9 system, which facilitates faster CO_2 reduction. The lower CO_2 feed in the R = 9 system allows for the rapid consumption of CO_2 molecules, while the higher CO_2 feed at R = 4 slows down the overall conversion process, resulting in a longer consumption time.

Fig. 3a–e demonstrates the evolution of the number of molecules of each major surface species with time at 500 K, 600 K, 700 K, 800 K and 900 K, respectively. The main products and key intermediates throughout the reaction include H_2O, H_2CO, H_3CO and HCO. At higher temperatures (700–900 K), a large number of H_2O molecules is produced in the early reaction stage, with some decomposing gradually as the reaction progresses, leading to a decrease in their number. In contrast, the production of H_2CO is significantly higher than that of H_3CO and HCO, while HCO is produced in the least amount, which shows high instability. The low stability of HCO may lead to its rapid consumption or transformation into other products. At 500 K, H_2CO showed some stability in the late stage of the reaction (800 ps–1000 ps), however, as the temperature increased, H_2CO decomposed more readily

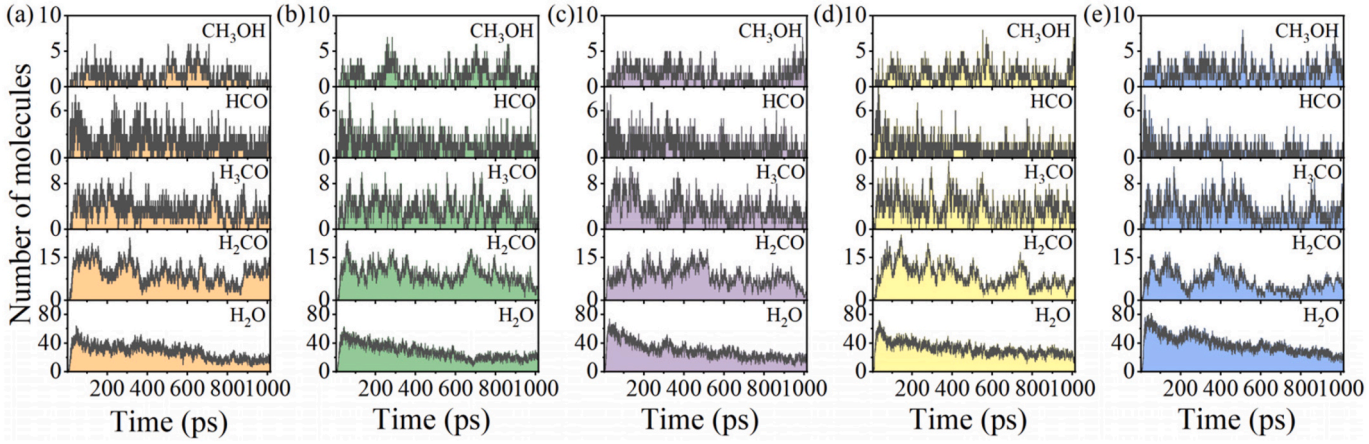

Fig. 3. Temporal evolution of the number of key species during the reaction on the Cu surface at (a) 500 K (b) 600 K (c) 700 K (d) 800k (e) 900k for the simulated system with an input gas composition of R = 9(CO_2:H_2 = 100:1000).

and the number of molecules decreased gradually. Additionally, the number of CH_3OH molecules remained relatively stable throughout the reaction, indicating that methanol formation is relatively stable across the temperature range and not significantly influenced by temperature changes in this case.

As the temperature increases, the equilibrium of the water-gas shift (WGS) reaction tends to produce more H_2O, whereas the RWGS reaction favors the production of CO and H_2O, which may affect the selective production of methanol. Fig. 4 shows the trend in the number of molecules of the key intermediate species with time at different temperatures for a hydrogen-carbon ratio of R = 4. It indicates that the amount of methanol production and the dynamic trend change significantly with increasing temperature: the amount of methanol molecules produced is significantly higher at R = 4 than at R = 9, and the fluctuation of the number of molecules with time is smaller. This suggests that a higher CO_2 content, i.e., a hydrogen-to-carbon ratio (R = 4), stabilizes methanol production and enhances its efficiency under these conditions. However, this also leads to a limited increase in the overall net methanol production. Additionally, under R = 4 conditions, the number of H_2O molecules produced during the reaction is significantly higher than that under R = 9 conditions. As the reaction progresses, the decrease in H_2O molecule count is minimal, indicating that the decomposition of H_2O is limited and that H_2O is not being significantly incorporated into other reaction pathways. The persistent presence of H_2O may lead to catalyst deactivation, as it can competitively occupy active sites and hinder the adsorption of reactants. This highlights the need for further attention to be paid to the potential effects of H_2O on the overall reaction process, particularly in terms of catalyst deactivation.

The reaction network and pathways for the hydrogenation of CO_2 to methanol on the catalyst surface were further analyzed to provide a comprehensive understanding of the catalytic process. The initial phase of CO_2 hydrogenation to methanol on the catalyst surface contains a complex reaction network and multiple mechanistic pathways, as shown in Fig. 5. The CO_2/H_2 system reaction mainly follows the formyl pathway ($CO_2 + H_2 \rightarrow CO \rightarrow CHO \rightarrow CH_2O \rightarrow CH_3O \rightarrow CH_3OH$), with CO_2 first reacting through the RWGS to form CO (R1). The CO is then sequentially hydrogenated to form CHO (R2), followed by stepwise hydrogenation to produce CH_2O, CH_2O, and ultimately methanol (Fig. 5a). As can be seen in Fig. 5b, the hydrogenation of CO_2 initially starts by trapping H atoms in the H_2 molecule, which can be observed at about 3.1 ps. In addition to the formyl pathway, an extended formyl pathway ($CO_2 + H_2 \rightarrow CO \rightarrow CHO \rightarrow CH_2O_2 \rightarrow CH_2O \rightarrow CH_3O \rightarrow CH_3OH$) was identified. In this pathway, CHO is first converted to CH_2O_2, which is either deoxygenated to CH_2O or further hydrogenated to CH_3O_2. CH_3O_2 is subsequently hydrogenated to CH_3O and ultimately methanol. The third pathway is the CH pathway ($CO_2 + H_2 \rightarrow CH \rightarrow$ CHO), with an intermediate product of CH. CO_2 reacts with H_2 to form CH, which is oxidized to CHO, and then further hydrogenated to methanol.

On the other hand, analysis of the catalyst structure in the last frame of the simulation revealed catalyst lattice structure distortions and coking deactivation (e.g., $Cu_{216}H_{103}C_{11}O_{63}$, as shown in Fig. 14). These process analyses can provide insight into the catalyst deactivation mechanism, which will be examined in detail in section 3.4. The existence of these competing pathways indicates the complexity of the reaction kinetics at the catalyst surface, where hydrogenation reactions occur simultaneously with C–O bond cleavage processes, leading to the generation of multiple intermediates.

3.2. CO hydrogenation process and reaction pathways

As shown in Eq. (2), CO is a key intermediate produced from CO_2 via the RWGS reaction and participates in the subsequent hydrogenation steps as one of the intermediates in the methanol synthesis pathway. Therefore, further study of the CO/H_2 system can reveal the interaction between CO and H_2 and its subsequent hydrogenation pathway, thus clarifying the role and influence of CO in the CO_2 hydrogenation system. As illustrated in Fig. 6, the temporal progression of the number of molecules of each major reaction product on the Cu surface is demonstrated at varying temperatures (500 K, 600 K, 700 K, 800 K, and 900 K) under a $CO:H_2$ ratio of 100:1000. The number of CO molecules decreases rapidly in the initial stage of the reaction, with the main observed intermediates being CH, H_2CO, and H_3CO. The consumption of H_2 increases significantly with temperature. However, the production of these intermediates is significantly lower in the CO hydrogenation system compared to the CO_2 hydrogenation system. At 500 K and 600 K, the methanol yields are very low and almost insignificant; at 700 K, the methanol production increases and peaks at about 4–5 molecules; at 800 K and 900 K, the methanol production fluctuates considerably, but the overall methanol yield increases.

In addition, in the CO_2/H_2 system, methanol production is greatly enhanced by intermediates (e.g., H_2CO) generated through CO_2 hydrogenation. However, this process also results in the generation of larger amounts of H_2O compared to the CO/H_2 system. The WGS reaction in the CO/H_2 system is relatively weak, and a single molecule of CO_2 is observed only on rare occasions. Furthermore, key intermediates such as H_2CO and H_3CO, along with H_2O, are produced in significantly smaller amounts compared to the CO_2/H_2 system, resulting in lower overall methanol yields. This indicates that although the CO_2/H_2 system generates a significant amount of CO and H_2O through the RWGS reaction, hydrogenation of CO alone may not be as efficient in producing large quantities of methanol. Unlike the direct hydrogenation of CO_2, the

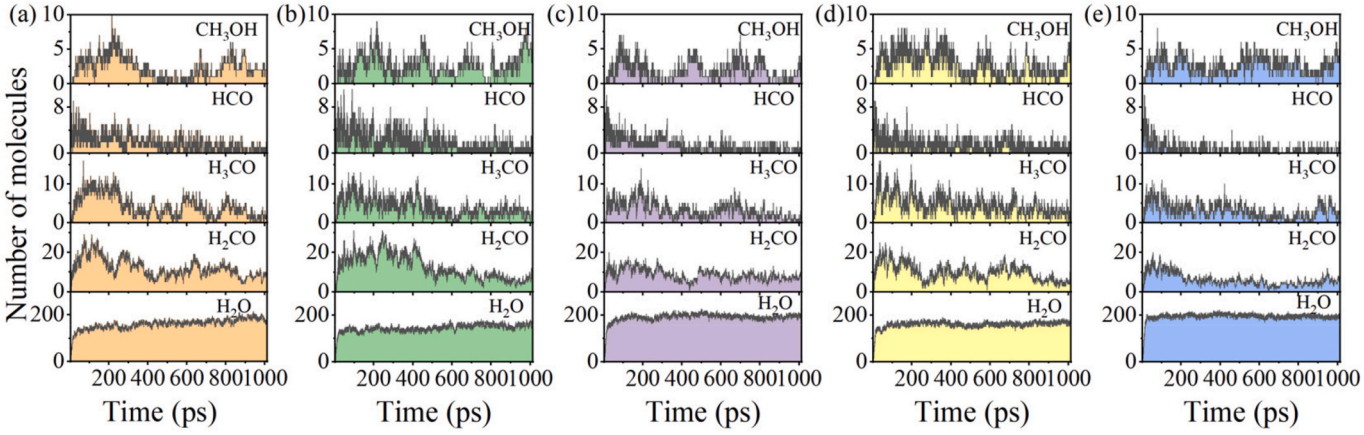

Fig. 4. Temporal evolution of the number of key species during the reaction on the Cu surface at (a) 500 K (b) 600 K (c) 700 K (d) 800k (e) 900k for the simulated system with an input gas composition of R = 4(CO_2:H_2 = 200:1000).

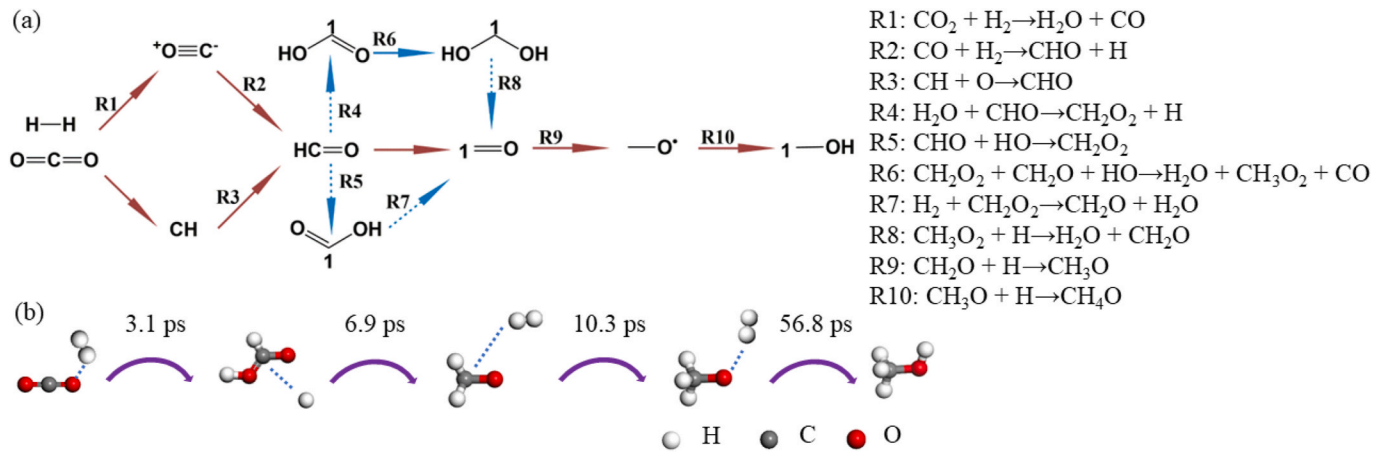

Fig. 5. Methanol production in the CO_2/H_2 system (a) Main reaction paths and intermediate products in the initial stage of the reaction on the catalyst surface. (b) Visual real-time trajectory showing the reaction process of CO_2 and H_2 reaction to produce methanol.

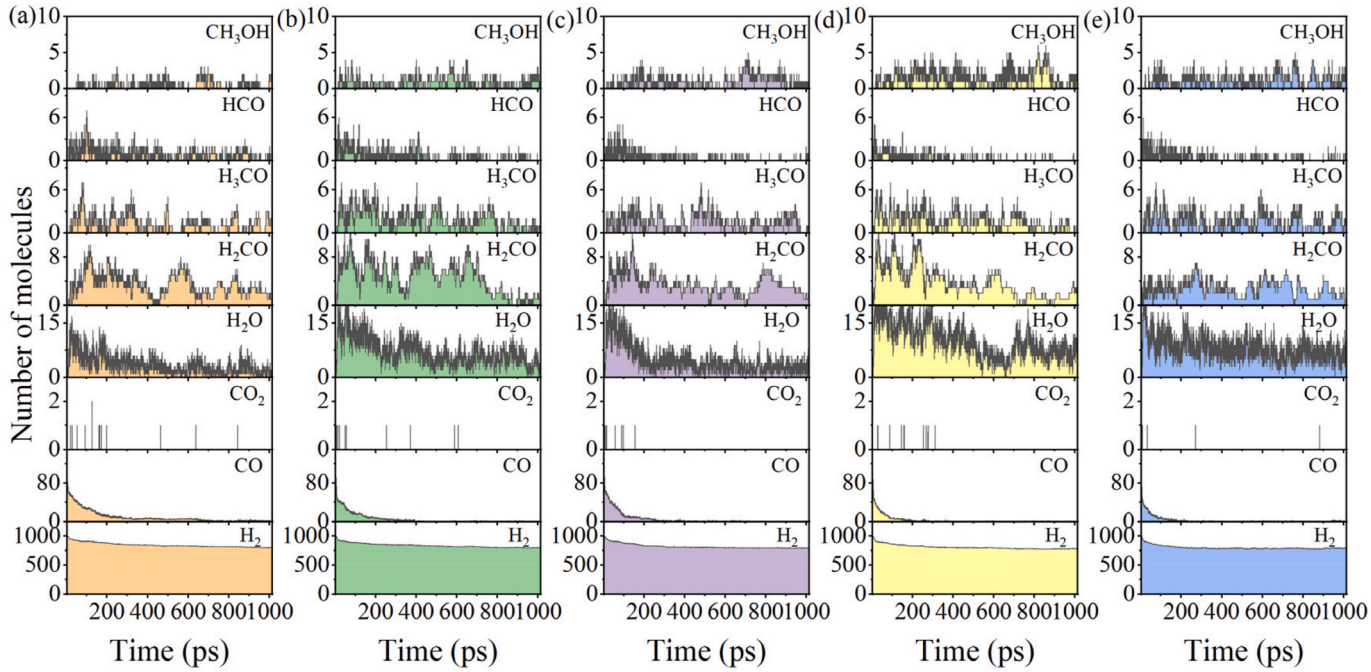

Fig. 6. Temporal evolution of the number of key species during the reaction on the Cu surface at (a) 500 K (b) 600 K (c) 700 K (d) 800k (e) 900k for the simulated system with an input gas composition of $CO:H_2 = 100:1000$.

adsorption and reactivity of CO on the Cu surface are somewhat limited. In the absence of CO_2 as a precursor, the hydrogenation rate of CO is relatively low, and its conversion pathway is not as efficient as that of CO_2 hydrogenation, resulting in a lower methanol yield in the CO/H_2 system.

Similar to the CO_2 hydrogenation pathway, CO hydrogenation mainly follows the formyl pathway, where HCO undergoes sequential hydrogenation to form CH_2O, CH_3O and other intermediates. However, apart from this main pathway, another reaction pathway can be observed where CO reacts with H_2 to form CH intermediates, followed by further hydrogenation to form CH_2 and CH_3. Ultimately, these intermediates can either combine with hydroxyl groups to form methanol or continue to react with H_2 to form CH_4. Fig. 7b demonstrates the evolution of the molecular structure of each key intermediate at different times during CO hydrogenation; Fig. 7c further shows the dynamic reaction process for the final formation of CH_3OH and CH_4. The observation of these pathways indicates that the CO hydrogenation reaction has multiple parallel pathways, with significant differences in the rate and stability of intermediate and product generation for each pathway. At the Cu surface, HCO is highly unstable and decomposes rapidly into CO and H atoms, with typically negligible or very low energy barriers. This instability hinders the $HCO^*+H^* \rightarrow H_2CO^*$ step in the formyl pathway of CO hydrogenation to methanol, thereby reducing catalytic activity.

3.3. CO_2/CO mixture hydrogenation process and reaction pathways

Studies of the CO_2/H_2 system have shown that CO is an inevitable byproduct in the hydrogenation of CO_2 to methanol, and its presence may influence the reaction pathway. To explore the effects of both CO_2 and CO in the reaction process when they coexist, their synergistic effects were analyzed. Based on this, a detailed study was conducted on a mixed syngas system containing both CO_2 and CO, with hydrogen-to-carbon ratios of R = 9.5 ($CO_2:CO:H_2 = 50:50:1000$) and R = 4.75

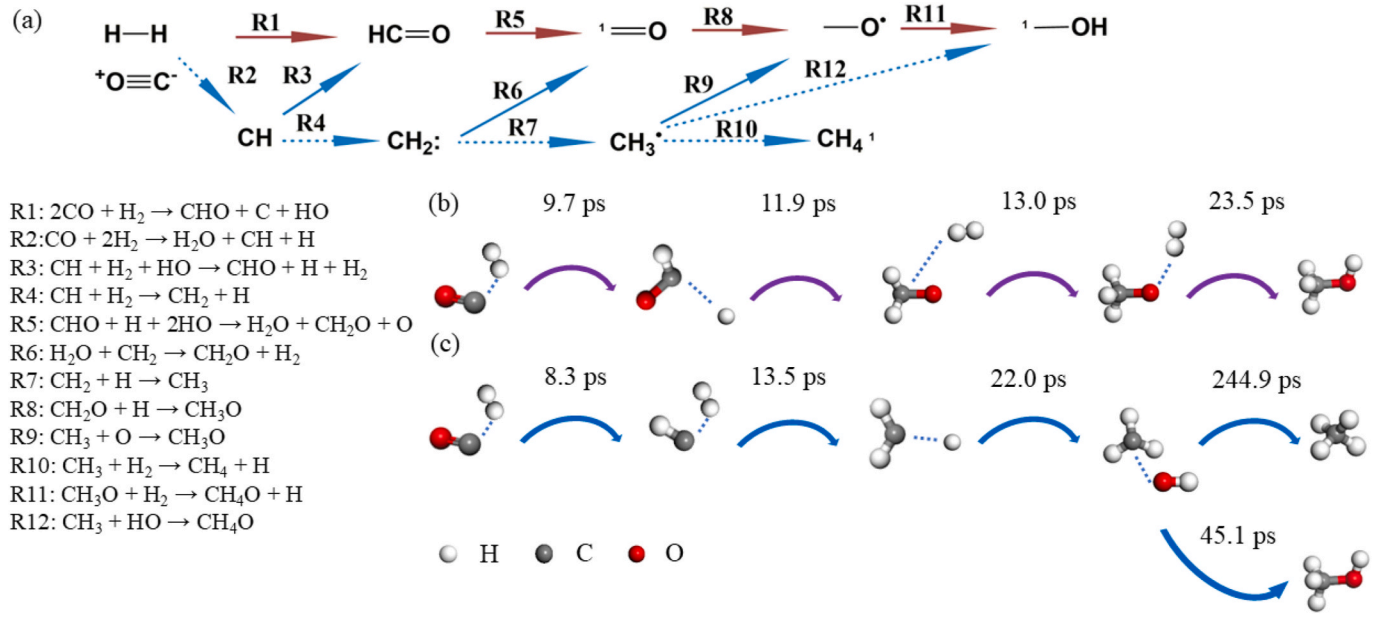

Fig. 7. Methanol production in the CO/H_2 system (a) Main reaction paths and intermediate products in the initial stage of the reaction on the catalyst surface. (b) Visual real-time trajectory showing the reaction process of CO and H_2 reaction to produce methanol. (c) The real-time trajectory of the reaction CO + $4H_2$ → CH_4 + H_2O.

(CO_2:CO:H_2 = 50:150:1000), to investigate their influence on intermediate species formation, product distribution, and overall reaction efficiency under conditions with the same carbon content.

Fig. 8 shows the distribution and molecular number evolution of the products during the reaction on the Cu catalyst surface at different temperatures. CO_2 reacts faster in the early reaction stage and is almost completely consumed within 50–100 ps. The rate of CO_2 consumption is slower at R = 4.75 compared to R = 9.5. On the other hand, CO consumption increased with temperature and was completely consumed at approximately 900 ps at the higher temperature (900 K), whereas CO was not fully consumed at R = 4.75. H_2 consumption was similar to that of the CO_2/H_2 system at R = 9.5, but in the CO_2/CO/H_2 system, the R = 4.75 condition consumed less hydrogen compared to the R = 4 condition for the CO_2/H_2 system. A comparative analysis of the molecular

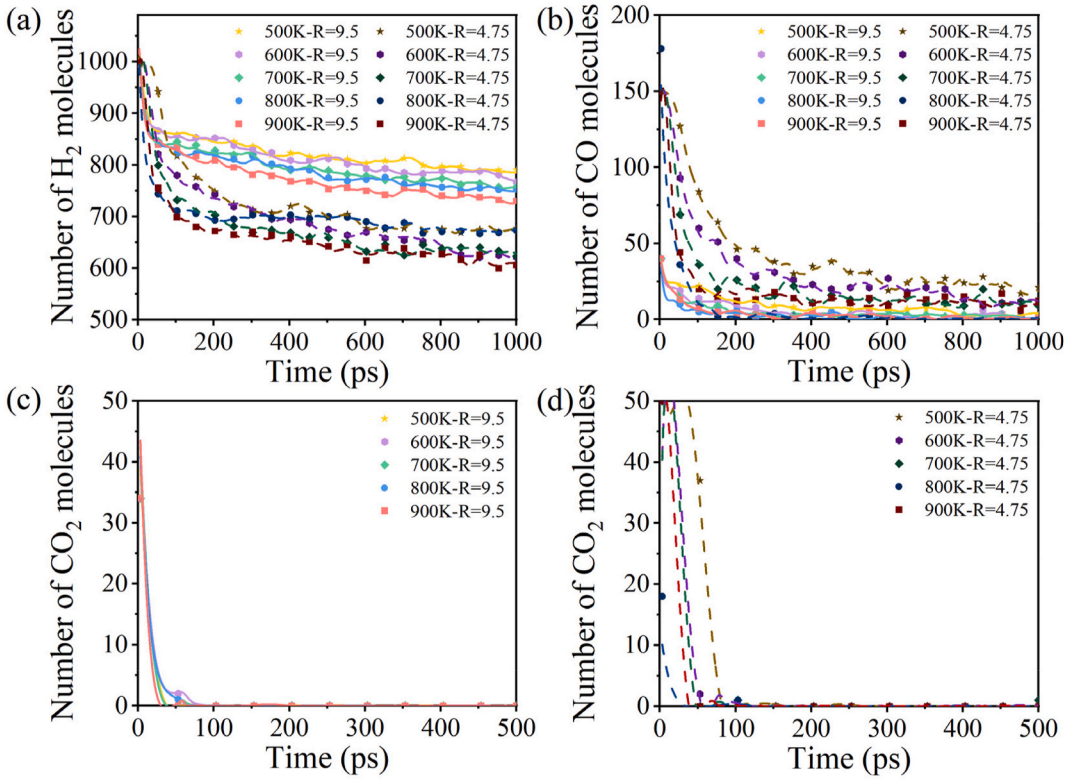

Fig. 8. Temporal evolution of the number of key species during the reaction on the Cu surface for input gas compositions R = 9.5 (CO_2:CO:H_2 = 50:50:1000) and R = 4.75 (CO_2:H_2 = 50:150:1000): (a) H_2 consumption (b) CO production (c) CO_2 consumption for R = 9.5 (d) CO_2 consumption for R = 4.75.

structure and bonding energy reveals that the C–O bond in the CO molecule has a bond length of 113 p.m. and a bond energy of 1072 kJ/mol, whereas the C–O bond in the CO_2 molecule has a bond length of 116 p.m. and a bond energy of 803 kJ/mol. Accordingly, the C–O bond of CO_2 is more susceptible to rupture, thereby facilitating the formation of novel reactive species. This renders CO_2 more amenable to participation in the reaction, ultimately leading to the generation of products such as methanol.

It has been established that an excessively elevated hydrogen-to-carbon ratio results in a substantial accumulation of H_2 within the reactor. Conversely, a hydrogen-to-carbon ratio that is insufficiently low increases the probability of side reactions, leading to an excessive accumulation of CO and CO_2. Consequently, the hydrogen-to-carbon ratio was optimized, and the variation in methanol yield at R = 4.75 (CO_2:CO:H_2 = 50:50:1000) was further analyzed, as illustrated in Fig. 9. At a hydrogen-to-carbon ratio of R = 4.75 and a temperature of 500 K, the lower hydrogen-to-carbon ratio led to an increase in the formation of H_2O molecules, along with an increase in intermediates such as H_2CO and H_3CO. The addition of more CO is therefore more favorable for the formation of key intermediates in the methanol synthesis pathway. Furthermore, at R = 4.75, the number of H_2O molecules did not decrease significantly but rather increased with rising temperature. However, at higher temperatures, the concentrations of key intermediates, such as H_2CO, H_3CO, and HCO, decreased significantly. The variation of these intermediates with time at different temperatures is shown in Fig. S1 and S2. These observations indicate that under the CO_2/CO mixture condition with R = 4.75 (higher CO content), CO consumes more H_2. The addition of an appropriate amount of CO promotes the WGS reaction, which consumes H_2O molecules. However, an excess of CO and elevated temperatures results in altered reaction pathways, with the RWGS reaction contributing directly to H_2O production or CO hydrogenation proceeding via CO + H → HCO → H_2O.

Maintaining an appropriate hydrogen to carbon ratio in a system where both CO and CO_2 are present promotes the continuation of the reaction in a sustained and efficient manner. As shown in Fig. 10, high R-value (H_2-dominated) conditions can significantly improve the methanol selectivity, but the demand for H_2 is higher, which may increase the economic cost of the reaction. Whereas, under low R-value (high carbon source concentration) conditions, the methanol selectivity remained low due to side-reaction competition and intermediate product accumulation. This phenomenon is mainly due to the limited activity of Cu-based catalysts in different reaction paths. The CO/H_2 system is less efficient in methanol generation and is more suitable as an intermediate research system.

The participation of CO under certain conditions (e.g., R = 9.5) can enhance the synergistic effect within the system and improve the selectivity of methanol generation. However, when the CO concentration is too high (e.g., R = 4.75), more H_2O is produced, which consumes some of the H_2 and reduces the efficiency of methanol generation (Fig. 10c). Whereas at higher carbon source concentrations (R = 4 and R = 4.75), the single CO_2/H_2 system resulted in higher H_2O generation due to the significant occurrence of the RWGS reaction, in the CO_2/CO/H_2 system, the introduction of CO can inhibit the overproduction of the RWGS reaction and thus reduce the H_2O generation. This synergism optimizes the carbon source utilization efficiency to a certain extent and enhances the overall reaction performance of the system.

3.4. *Effect of H_2O on the CO_2 hydrogenation process and reaction pathways*

During the CO_2 hydrogenation process, H_2O is inevitably formed as a by-product. The generated H_2O can participate in the RWGS reaction, leading to the coverage or alteration of active sites on the catalyst surface, which accelerates catalyst oxidation and deactivation. To explore the influence of H_2O on reaction kinetics and intermediate distribution in CO_2 hydrogenation, a system incorporating H_2O (CO_2:H_2: H_2O = 100:940:60) was designed to evaluate its impact on the RWGS reaction and the overall reaction mechanism. As shown in Fig. 11 and Supplementary Fig. S3, the consumption of H_2 exhibited a notable increase in the system with the addition of H_2O compared to the R = 9 system without the addition of H_2O. In addition, the stable presence and high concentration of CO during the reaction indicate that the introduction of H_2O significantly affects the kinetic process of the RWGS reaction, which in turn has an impact on the reaction mechanism and the distribution of intermediates in CO_2 hydrogenation.

As shown in Fig. 12a, the introduction of a small amount of H_2O molecules at 500 K resulted in a significant increase in methanol selectivity compared to the CO_2/H_2 system, and the overall yield of methanol was higher than that in the CO_2/H_2 system at R = 8.4. This indicates that the presence of H_2O plays a positive role in promoting methanol production, likely due to its involvement in enhancing the hydrogenation reaction efficiency. Further analyses showed that there were significant differences in the effect on methanol yield at different temperatures, as shown in Fig. 12b. Although the methanol yield occasionally reached 6 % in the range of 600 K–900 K, overall the methanol yield showed a more stable trend at 500 K and 600 K. The methanol

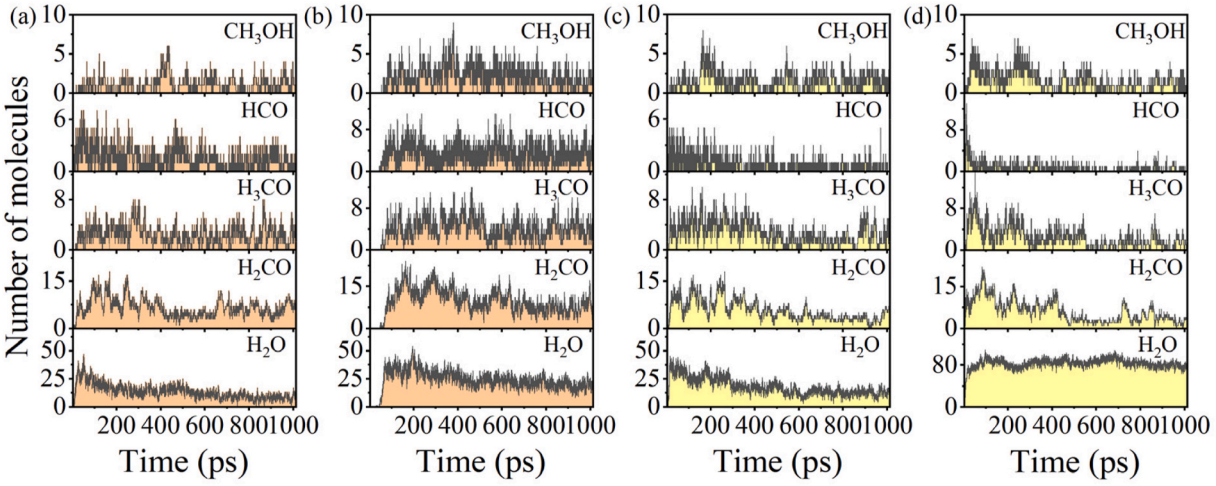

Fig. 9. Temporal evolution of key species during Cu surface reactions at different temperatures and gas compositions: (a) 500 K with an input gas composition of R = 9.5(CO_2:CO:H_2 = 50:50:1000) (b) 500 K with an input gas composition R = 4.75(CO_2:CO:H_2 = 50:150:1000) (c) 800 K with gas composition R = 9.5(CO_2:CO:H_2 = 50:50:1000) and (d) 800 K with an input gas composition R = 4.75(CO_2:CO:H_2 = 50:150:1000).

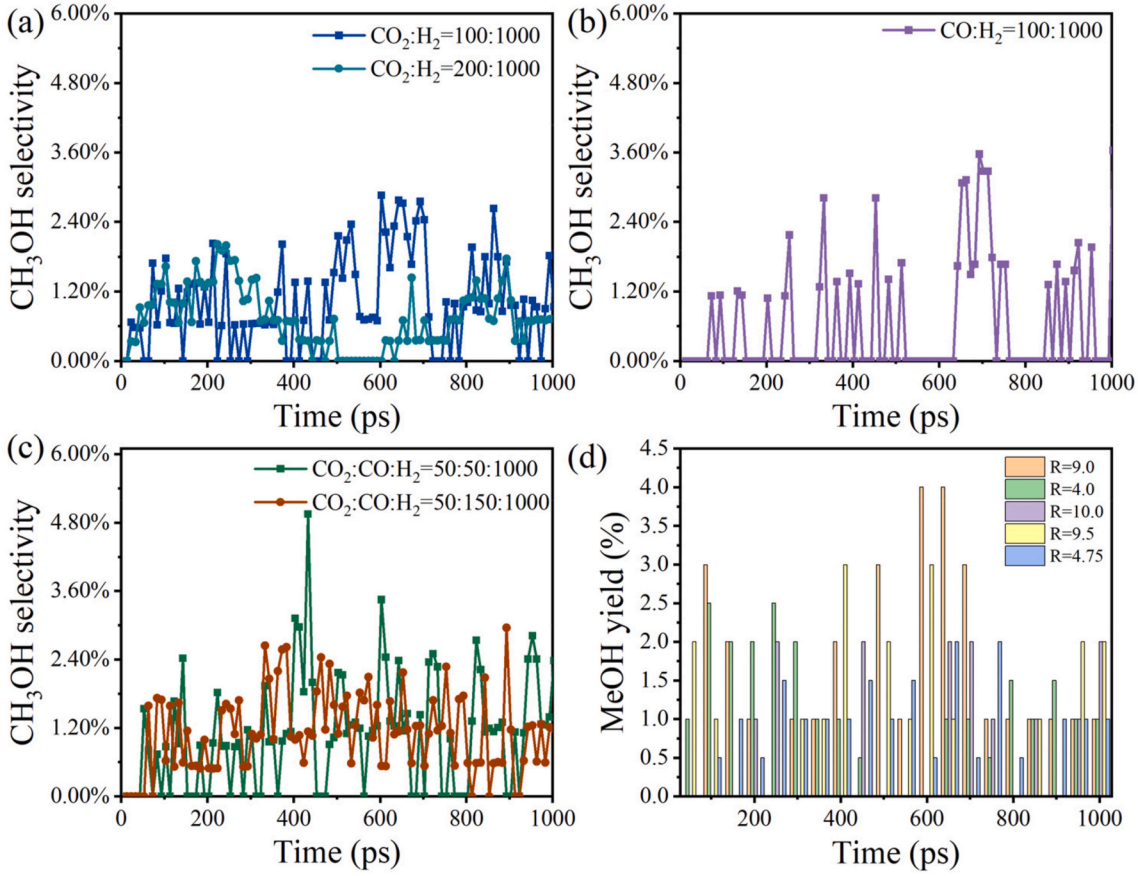

Fig. 10. Methanol selectivity at varying hydrogen-to-carbon ratios. (a) CO_2/H_2 system with hydrogen-to-carbon ratios of R = 9 and R = 4. (b) CO/H_2 system with a hydrogen-to-carbon ratio of R = 10. (c) $CO_2/CO/H_2$ system with a hydrogen-to-carbon ratio of R = 9.5 and R = 4.75. (d) Methanol yield.

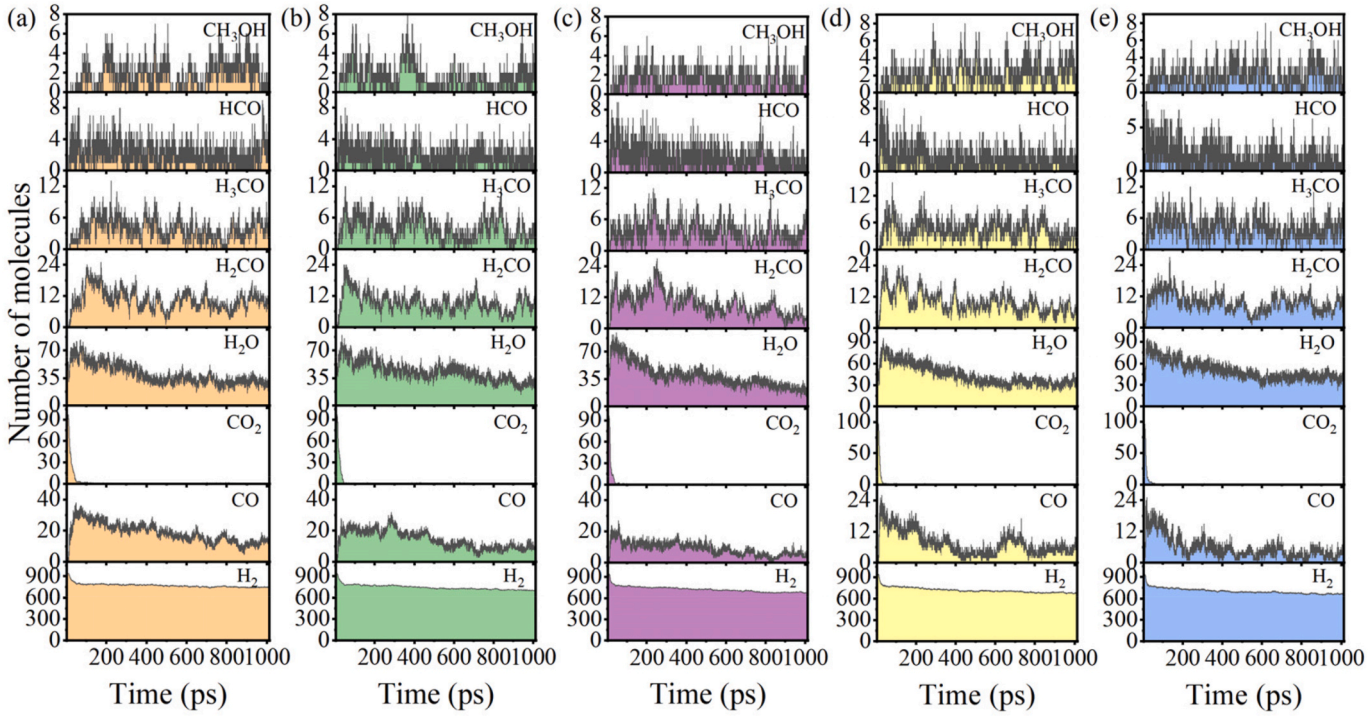

Fig. 11. Temporal evolution of the number of key species during the reaction on the Cu surface at (a) 500 K (b) 600 K (c) 700 K (d) 800k (e) 900k for the simulated system with an input gas composition of CO_2:H_2: H_2O = 100:940:60.

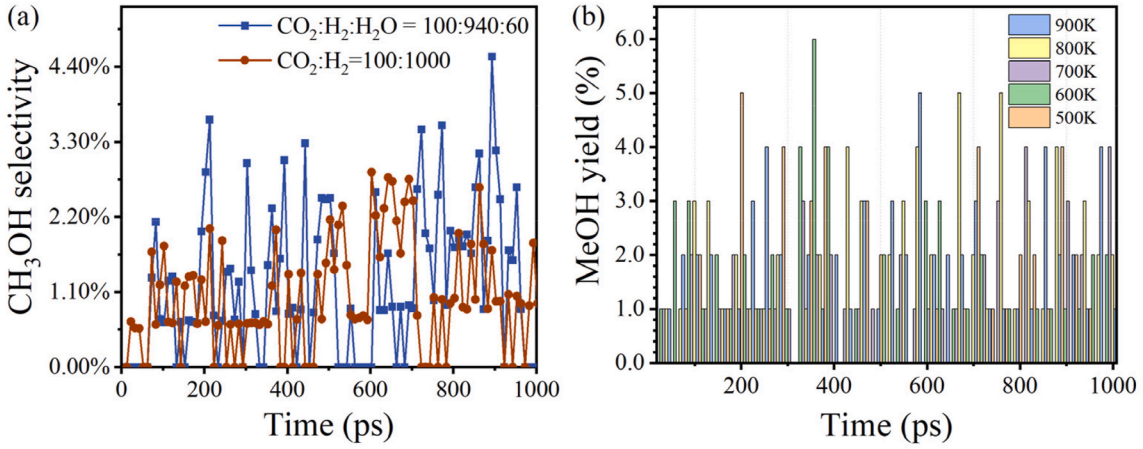

Fig. 12. Input gas composition hydrogen-carbon ratio R = 8.4 ($CO_2/H_2/H_2O$) system (a) Methanol selectivity (b) Methanol yield.

yield at 500 K and 600 K was also higher than the methanol yield at 600 K. These results indicate that the appropriate temperature and the presence of H_2O are important for improving the methanol production efficiency. They also demonstrate that the addition of small amounts of H_2O molecules, while not significantly increasing the methanol production rate, can influence the reaction pathway and product distribution by consuming more H_2 and altering the distribution of intermediate products.

Based on the available results indicating that the introduction of a small amount of H_2O molecules helps to enhance the selectivity and yield of methanol, the reaction path of CO_2 hydrogenation to methanol on the catalyst surface was analyzed to obtain another key reaction path. As shown in Fig. 13, similar to the main reaction path of the CO_2/H_2 system, CO_2 is first reduced to CO, which is subsequently hydrogenated step by step to produce HCO, H_2CO, H_3CO, and finally methanol. The other critical path (R9) is $CH_3O + H_2O \rightarrow CH_4O + HO$, where methoxy ($CH_3O$) reacts with externally introduced H_2O on the catalyst (methoxy hydrolysis) instead of reacting with H_2 (methoxy hydrogenation) to produce methanol. The conversion of methoxy to methanol in the hydrolysis reaction and the introduction of externally-introduced H_2O opens up this critical pathway, which improves the efficiency of the conversion of CO_2 to methanol. However, this pathway was only observed in systems where a small amount of externally introduced H_2O was present, but not in pure CO_2/H_2 or $CO_2/CO/H_2$ systems. Externally introduced H_2O molecules are more likely to participate in the hydrolysis reaction due to their diffusive behavior or distribution properties, whereas H_2O generated by the RWGS reaction may not effectively trigger the pathway due to its uneven distribution or limited diffusion. This process was significantly affected by the H_2O diffusion efficiency, the structural stability of the Cu catalysts, and the inhibition of C accumulation.

Since the deactivation of Cu catalysts and its induced active site changes play a key role in the methanol synthesis process, we observed and analyzed the structure of Cu catalysts at the end of the reaction (i.e., at the moment of 1000 ps). Fig. 14 shows the structural morphologies of Cu catalysts in the CO_2/H_2, CO/H_2, $CO_2/CO/H_2$ and $CO_2/H_2/H_2O$ systems. It was found that in the $CO_2/H_2/H_2O$ system, the C content on the catalyst surface was significantly lower than that of the other three systems, indicating that the C build-up had a lesser effect on the Cu catalyst. In the CO/H_2 system, the CO was more easily adsorbed on the Cu surface, which led to a large accumulation of C atoms and the number of accumulated C was as high as 70, resulting in a severe deactivation of the catalyst and the generation of the least number of methanol molecules.

To further investigate catalyst deactivation, we analyzed Cu–C and C–O interactions via RDF analysis (Fig. S4). In the CO_2/H_2 and $CO_2/H_2/H_2O$ reaction systems, the RDF reveals pronounced C–O peaks, indicating the predominance of oxygenated carbon species, such as carbonates or formates, on the Cu surface. These species usually exist in the form of adsorbed intermediates, which are closely related to the catalytic process. In contrast, in the CO/H_2 and $CO_2/CO/H_2$ systems, the RDF exhibits higher Cu–C peaks, suggesting that the carbon atoms are more inclined to form chemical bonds directly with the Cu surface. This enhanced Cu–C interaction suggests that carbon is more likely to be

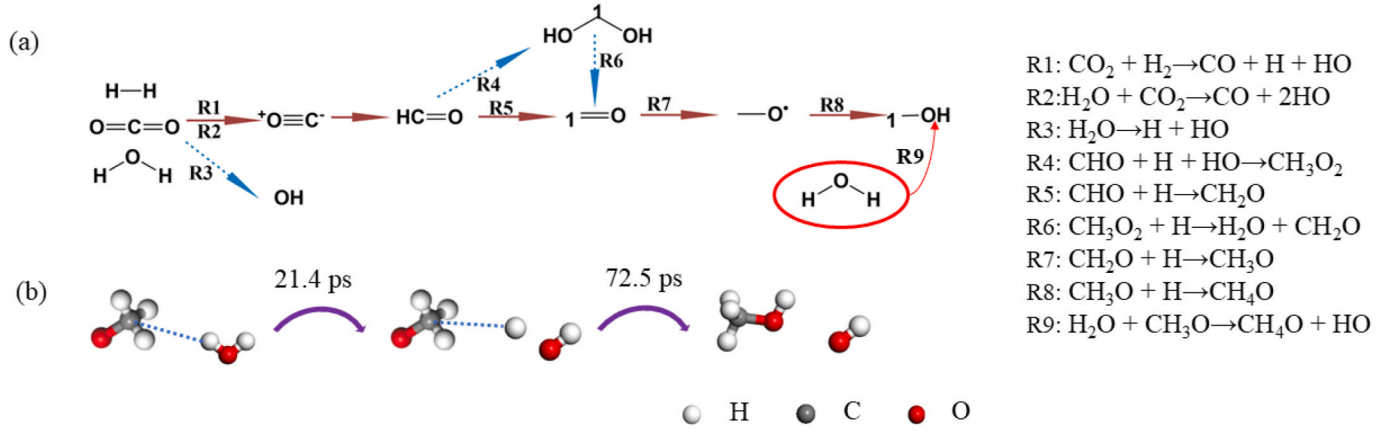

Fig. 13. Methanol production in the $CO_2/H_2/H_2O$ system (a) Main reaction paths and intermediate products in the initial stage of the catalyst surface reaction for the $CO_2/H_2/H_2O$ system. (b) The real-time trajectory of the reaction $CH_3O + H_2O \rightarrow CH_4O + HO$.

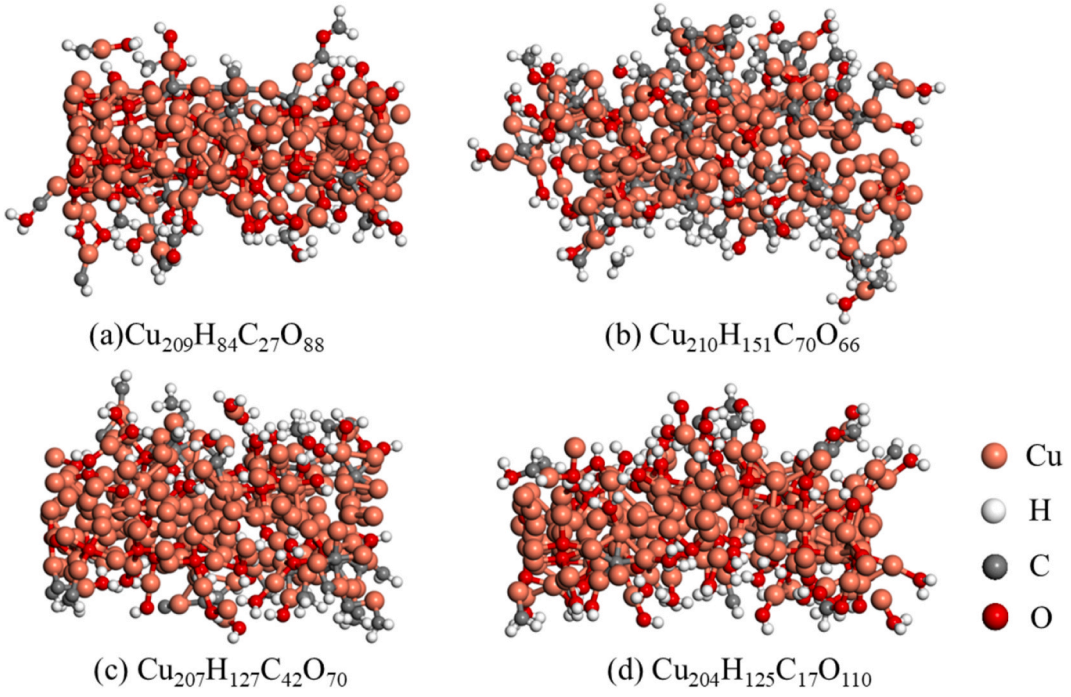

Fig. 14. Schematic representation of the final structure of the Cu catalyst in different reaction systems at 500 K temperature. (a) CO_2:H_2 = 100:1000 (b) CO:H_2 = 100:1000 (c) CO_2:CO:H_2 = 50:50:1000 (d) CO_2:H_2:H_2O = 100:940:60.

deposited on the Cu surface in these systems, thus covering the active sites. Fig. 14 illustrates the trend of carbon content across different reaction systems, corroborating the RDF analysis. The intensity of the Cu–C peaks is positively correlated with the degree of carbon coverage on the Cu surface. The results showed that the introduction of an appropriate amount of H_2O molecules into the reaction system can effectively inhibit the formation of C deposits and maintain the activity of the catalyst, thus promoting the methanol generation.

3.5. Reaction rate assessment of CO_2 hydrogenation

Based on the above ReaxFF results, a kinetic analysis was conducted to analyze the reaction rates of the basic steps. The hydrogenation of carbon dioxide to methanol is typically performed in a hydrogen-rich environment at temperatures between 473.15 K and 623.15 K, where both high reactivity and catalyst stability are achieved. To closely replicate typical reaction conditions, the following conditions were selected for the kinetic analysis: CO_2:H_2 = 100:1000, CO:H_2 = 100:1000, CO_2:H_2: H_2O = 100:940:60, all at 500 K. As illustrated in Table 2, a comprehensive analysis of the reaction pathways involved in the conversion of CO_2 to methanol was conducted via the intermediate steps. This analysis revealed significant disparities in the kinetic parameters and activation energies associated with these processes. The initial reaction step R1, with an activation energy of 61.95 kJ/mol and a reaction rate of $3.37 \times 10^6\ s^{-1}$, is the critical starting point of the whole reaction sequence. The key step R14, which ultimately generates methanol, has an activation energy of 53.78 kJ/mol, indicating that this step has an important role in the methanol synthesis process. In CO_2 hydrogenation reactions, multiple reaction paths compete to proceed, with the path with the lowest activation energy typically dominating the reaction. A comprehensive analysis of the activation energies of the steps reveals that the activation energies of the intermediate steps in the methanol synthesis pathway range from 45.09 kJ/mol to 62.89 kJ/mol. Among the aforementioned steps, R2 represents the key rate-limiting step, whereby CO reacts with H_2 to form CHO and H. This step exerts a significant influence on the overall reaction rate.

To test the accuracy of the ReaxFF force field parameters in the current system, our calculated results are compared with the DFT calculations and some experimental results in the literature. Zhao et al. [18] investigated the activation energies of the reactions $H_2CO(g) + H \leftrightarrow H_2COH$ and $H_2COH + H \leftrightarrow H_3COH$ for Cu(111) catalysts. The activation energies were found to be 67.54 kJ/mol and 63.68 kJ/mol, respectively, which correspond to the activation energies of the reactions R12 (51.62 kJ/mol) and R13 (62.89 kJ/mol) as listed in Table 2. Experimental results [51,52] further indicate apparent activation energies of 68 kJ/mol for Cu/ZnO/Al_2O_3, 52 kJ/mol for Cu/ZnO/ZrO_2, and 105 kJ/mol for Cu(111) catalysts. As shown in Table 2, reaction steps R1, R2, R12, R14, and R15 were key rate-determining steps in the mechanism. In multistep reactions, the overall activation energy is usually determined by the activation energy of the rate-limiting step. Thus, in the CO_2/H_2 system the overall activation energy is determined by the rate-determining step, denoted as R15, which has an activation energy of 94.98 kJ/mol. These values are consistent with our ReaxFF

Table 2
Elementary steps and reaction rates for CO_2:H_2 = 100:1000 at 500 K.

Reaction steps	Reaction rate (s^{-1})	order of reaction	Ea (kJ/mol)
$CO_2 + H_2 \rightarrow H_2O + CO$	R1: 3.37E+06	1	61.95
$CO + H_2 \rightarrow CHO + H$	R2: 4.78E+05	1	70.07
$CH + O \rightarrow CHO$	R3: 1.14E+08	1	57.57
$H_2O + CHO \rightarrow CH_2O_2 + H$	R4: 1.09E+08	1	46.02
$CHO + HO \rightarrow CH_2O_2$	R5: 1.84E+08	1	45.33
$CH + 2HO \rightarrow CH_2O_2 + HO$	R6: 8.43E+06	1	58.14
$H_2 + CH_2O_2 \rightarrow CH_2O + H_2O$	R7: 1.95E+08	1	45.09
$CH_3O_2 + H \rightarrow H_2O + CH_2O$	R8: 6.48E+09	2	30.52
$CH_3O + H \rightarrow CH_2O + H_2$	R9: 1.09E+09	1	37.93
$CH_2O_2 + CH_2O + HO \rightarrow H_2O + CH_3O_2 + CO$	R10: 2.19E+06	1	63.74
$CH_2O + CH_2O \rightarrow CH_3O_2 + CH$	R11: 2.90E+08	1	43.44
$CH_2O + H \rightarrow CH_3O$	R12: 4.05E+07	2	51.62
$CH_2O + H_2 \rightarrow CH_3O + H$	R13: 2.69E+06	1	62.89
$CH_3O + H \rightarrow CH_4O$	R14: 2.41E+07	1	53.78
$CH_3O + H_2 \rightarrow CH_4O + H$	R15: 1.19E+03	1	94.98
$H_2O \rightarrow H + HO$	R16: 1.02E+09	2	38.22
$H + HO \rightarrow H_2O$	R17: 3.47E+07	2	52.26

MD calculations, with differences within acceptable computational and experimental error ranges. This consistency validates the applicability of the ReaxFF force-field for modeling CO_2 hydrogenation over Cu catalysts.

Table 3 lists the elementary steps and corresponding reaction rates for the CO:H_2 = 100:1000 system at 500 K. The initial reaction steps, including the dissociation of CO into C and H (R1), the formation of CH and H (R2), and the production of H_2O and C (R3), have activation energies ranging from 61.21 kJ/mol to 68.66 kJ/mol, and serve as the crucial initiation steps for the system. Subsequent steps (e.g., R10 and R11) involve the reactions of intermediates like CH_2O and CH_3O, with activation energies showing a gradual decrease. This indicates that the reaction rate accelerates as the reactivity of the intermediates increases. In addition, since CO adsorbs more readily on Cu surfaces, its decomposition (R1, R3) leads to significant C deposition.

In the $CO_2/H_2/H_2O$ system, the primary reaction pathway proceeds through the formation of CO and HO radicals, as indicated by the high reaction rates of R1 (2.86×10^6 s^{-1}) and R2 (1.01×10^8 s^{-1}) (see Table 4). The reaction step R14 ($CH_4O \rightarrow CH_3O + H$) had a high reaction rate of 6.76×10^9 s^{-1} and an activation energy of 30.35 kJ/mol, which is the lowest among all the steps. The decomposition of CH_4O to CH_3O radicals is a highly favorable and rapid process, which may significantly impact the overall efficiency of methanol formation. H_2O molecules are actively involved in several reaction steps, including R2, R7, R8, R12, R16, R17, and R18. Among them, R18 ($H_2O \rightarrow H + HO$) has a high reaction rate (1.59×10^9 s^{-1}) and a low activation energy (36.36 kJ/mol), indicating that the decomposition of H_2O is a fast and efficient process that generates HO radicals. These processes not only demonstrate the important influence of H_2O on the reaction pathway, but also suggest that H_2O plays a key role in facilitating the selective production of methanol.

Table 3
Elementary steps and reaction rates for CO:H_2 = 100:1000 at 500 K.

Reaction steps	Reaction rate (s-1)	order of reaction	Ea (kJ/mol)
$CO + H_2 \rightarrow C + H + HO$	R1: 4.03E+06	1	61.21
$CO + H_2 \rightarrow CH + H + O$	R2: 6.71E+05	1	68.66
$CO + H_2 \rightarrow H_2O + C$	R3: 1.34E+06	1	65.78
$CH + O \rightarrow CHO$	R4: 2.74E+08	1	43.67
$CH + HO \rightarrow CH_2O$	R6: 4.05E+07	2	47.11
$CH_2O_2 + CH \rightarrow CH_3O_2 + C$	R7: 2.23E+08	1	44.53
$CH_2O + H_2O \rightarrow CH_3O_2 + H$	R8: 7.90E+07	1	48.84
$CH_3O_2 + CH \rightarrow CH_2O + C + H + HO$	R9: 1.51E+09	1	36.59
$CH_2O + H \rightarrow CH_3O$	R10: 4.44E+07	1	51.23
$CH_3O + H \rightarrow CH_4O$	R11: 6.73E+07	1	49.51
$H + HO \rightarrow H_2O$	R12: 1.97E+08	2	45.05
$H_2O \rightarrow H + HO$	R13: 1.12E+09	2	37.82

Table 4
Elementary steps and reaction rates for CO_2:H_2: H_2O = 100:940:60 at 500 K.

Reaction steps	Reaction rate (s^{-1})	order of reaction	Ea (kJ/mol)
$CO_2 + H_2 \rightarrow CO + H + HO$	R1: 2.86E+06	1	62.63
$H_2O + CO_2 \rightarrow CO + 2HO$	R2: 1.01E+08	2	57.38
$CO + H_2 \rightarrow CH + HO$	R3: 4.39E+05	1	70.42
$C + HO \rightarrow CHO$	R4: 7.48E+06	1	70.37
$CHO + H + HO \rightarrow CH_3O_2$	R6: 6.86E+06	1	59.00
$CH_3O_2 + H \rightarrow H_2O + CH_2O$	R7: 7.14E+08	2	39.69
$H_2O + CH_2 \rightarrow CH_2O + H_2$	R8: 1.55E+07	2	55.61
$CHO + H \rightarrow CH_2O$	R9: 2.04E+08	1	44.90
$CH_2O + H \rightarrow CH_3O$	R10: 2.44E+07	1	53.72
$CH_3O + H \rightarrow CH_4O$	R11: 1.89E+07	2	54.80
$H_2O + CH_3O \rightarrow CH_4O + HO$	R12: 1.02E+07	1	57.34
$CH_4O + CO \rightarrow CHO_2 + CH_3$	R13: 1.99E+08	1	45.00
$CH_4O \rightarrow CH_3O + H$	R14: 6.76E+09	1	30.35
$CH_4O + H \rightarrow H_2O + CH_3$	R15: 7.44E+07	1	49.09
$H_2O + CHO \rightarrow CH_2O_2 + H$	R16: 2.62E+08	2	43.86
$H_2O + H \rightarrow H_2 + HO$	R17: 7.79E+06	2	58.47
$H_2O \rightarrow H + HO$	R18: 1.59E+09	2	36.36

4. Conclusion

In this study, the hydrogenation of CO_2 to methanol on Cu surfaces was systematically investigated using ReaxFF MD simulations. The analysis focused on the effects of the hydrogen-to-carbon ratio, temperature, and the presence of CO and H_2O on the reaction pathways. Through a detailed examination of key intermediate species and kinetic studies, the mechanisms of individual reaction steps and their corresponding activation energies were elucidated. The main findings can be drawn as follows:

(1)The detail analysis of the CO_2 hydrogenation network shows that the main reaction pathway follows the formyl pathway ($CO_2 \rightarrow CO \rightarrow CHO \rightarrow CH_2O \rightarrow CH_3O \rightarrow CH_3OH$). In addition, an extended formyl pathway ($CO_2 + H_2 \rightarrow CO \rightarrow CHO \rightarrow CH_2O_2 \rightarrow CH_2O \rightarrow CH_3O \rightarrow CH_3OH$) was found. The third pathway is the CH pathway ($CO_2 + H_2 \rightarrow CH \rightarrow CHO$).

(2) In the CO/H_2 system, in addition to the formyl pathway, a new methane formation pathway ($CO + H_2 \rightarrow CH \rightarrow CH_2 \rightarrow CH_3 \rightarrow CH_4$) was identified, while significant carbon deposition simultaneously occurs, leading to reduced catalyst efficiency and lower methanol selectivity. The high activation energies of the initial reactions (R1 and R3) (61.21 kJ/mol and 65.78 kJ/mol, respectively) not only hinder the reaction rate but also promote carbon deposition on the catalyst.

(3) The incorporation of CO to a CO_2/H_2 system attenuates excessive RWGS reactions and minimizes H_2O production, thereby improving overall reaction efficiency and increasing methanol yield. Higher H_2 dominant conditions (high R-value) increase methanol selectivity, while lower R-values (higher carbon concentration) decrease methanol selectivity due to increased side reactions and intermediate accumulation.

(4) In the $CO_2/H_2/H_2O$ system, the introduction of a small number of external H_2O molecules improves the efficiency of CO_2 conversion to methanol via the methoxy hydrolysis pathway ($CH_3O + H_2O \rightarrow CH_4O + HO$). The presence of H_2O has been shown to significantly increase the reaction rates of the intermediates CH_2O and CH_3O, as evidenced by the high reaction rates of R9 (2.04×10^8 s^{-1}) and R10 (2.44×10^7 s^{-1}).

CRediT authorship contribution statement

Meirong Dong: Writing – review & editing, Writing – original draft, Resources, Project administration, Investigation, Formal analysis, Conceptualization. **Zehua Huang:** Writing – review & editing, Writing – original draft, Visualization, Validation, Formal analysis, Data curation. **Junchang Xiong:** Investigation, Formal analysis, Data curation, Conceptualization. **Hongchuan Liu:** Investigation, Formal analysis, Conceptualization. **Youcai Liang:** Investigation, Conceptualization. **Jidong Lu:** Methodology, Formal analysis, Conceptualization.

Declaration of competing interest

The authors declare that they have no known competing financial interests or personal relationships that could have appeared to influence the work reported in this paper.

Acknowledgements

The research was supported by the National Natural Science Foundation of China (No. 52376107) and Foundation of Science and Technology Projects in Guangzhou (2025A04J7048). We also acknowledge

the support from the Fundamental Research Funds for the Central Universities (2022ZFJH04) and Guangdong Province Key Laboratory of Efficient and Clean Energy Utilization (2013A061401005).

Appendix A. Supplementary data

Supplementary data to this article can be found online at https://doi.org/10.1016/j.ijhydene.2025.05.049.

References

[1] Li W, Li X, Song C, Gao G. Carbon removal, sequestration and release by mariculture in an important aquaculture area, China. Sci Total Environ 2024;927:172272.
[2] Whang HS, Lim J, Choi MS, Lee J, Lee H. Heterogeneous catalysts for catalytic CO_2 conversion into value-added chemicals. Bmc Chem. Eng. 2019;1:1–19.
[3] Ishaq H, Dincer I, Crawford C. A review on hydrogen production and utilization: challenges and opportunities. Int J Hydrogen Energy 2022;47:26238–64.
[4] Nie W, Dong M, Lu J. Simultaneous measurement of H_2O concentration and effective absorption optical path length under unknown optical path length condition based on a single spectral line. Spectrochim Acta Mol Biomol Spectrosc 2022;270:120774.
[5] Zhang X, Zhang G, Song C, Guo X. Catalytic conversion of carbon dioxide to methanol: current status and future perspective. Front Energy Res 2021;8:621119.
[6] Sonthalia A, Kumar N, Tomar M, Edwin Geo V, Thiyagarajan S, Pugazhendhi A. Moving ahead from hydrogen to methanol economy: scope and challenges. Clean Technol Environ Policy 2021;25:551–75.
[7] Tedeeva MA, Kustov AL, Batkin AM, Garifullina C, Zalyatdinov AA, Yang D, et al. Catalytic systems for hydrogenation of CO_2 to methanol. Mol Catal 2024;566:114403.
[8] Ye R, Xiao S, Lai Q, Wang D, Huang Y, Feng G, et al. Advances in enhancing the stability of Cu-based catalysts for methanol reforming. Catalysts 2022;12:747.
[9] Niu J, Liu H, Jin Y, Fan B, Qi W, Ran J. Comprehensive review of Cu-based CO_2 hydrogenation to CH_3OH: insights from experimental work and theoretical analysis. Int J Hydrogen Energy 2022;47:9183–200.
[10] Liang H, Zhang G, Li Z, Zhang Y, Fu P. Catalytic hydrogenation of CO_2 to methanol over Cu-based catalysts: active sites profiling and regulation strategy as well as reaction pathway exploration. Fuel Process Technol 2023;252:107995.
[11] Cui X, Chen S, Yang H, Liu Y, Wang H, Zhang H, et al. Improving methanol selectivity in CO_2 hydrogenation by tuning the distance of Cu on catalyst. Appl Catal B Environ 2021;298:120590.
[12] Zheng M, Zhang J, Wang P, Jin H, Zheng Y, Qiao SZ. Recent advances in electrocatalytic hydrogenation reactions on copper-based catalysts. Adv Mater 2024;36:2307913.
[13] J Q. A brief review on the reaction mechanisms of CO_2 hydrogenation into methanol. Int. J. Innovat. Res. Sci. Stud. 2020;2:53–63.
[14] Kunkes EL, Studt F, Abild-Pedersen F, Schlögl R, Behrens M. Hydrogenation of CO_2 to methanol and CO on $Cu/ZnO/Al_2O_3$: is there a common intermediate or not? J Catal 2015;328:43–8.
[15] Larmier K, Liao WC, Tada S, Lam E, Verel R, Bansode A, et al. CO_2-to-Methanol hydrogenation on zirconia-supported copper nanoparticles: reaction intermediates and the role of the metal–support interface. Angew Chem Int Ed 2017;56:2318–23.
[16] Tang C, Tang S, Sha F, Han Z, Feng Z, Wang J, et al. Insights into the selectivity determinant and rate-determining step of CO_2 hydrogenation to methanol. J Phys Chem C 2022;126:10399–407.
[17] Sharma P, Sebastian J, Ghosh S, Creaser D, Olsson L. Recent advances in hydrogenation of CO_2 into hydrocarbons via methanol intermediate over heterogeneous catalysts. Catal Sci Technol 2021;11:1665–97.
[18] Zhao Y, Yang Y, Mims C, Peden CHF, Li J, Mei D. Insight into methanol synthesis from CO_2 hydrogenation on Cu(111): complex reaction network and the effects of H_2O. J Catal 2011;281:199–211.
[19] Liu J, Ke Q, Chen X. First-principles investigation of methanol synthesis from CO_2 hydrogenation on Cu@Pd core–shell surface. J Mater Sci 2021;56:3790–803.
[20] Kalz KF, Kraehnert R, Dvoyashkin M, Dittmeyer R, Gläser R, Krewer U, et al. Future challenges in heterogeneous catalysis: understanding catalysts under dynamic reaction conditions. ChemCatChem 2017;9:17–29.
[21] Zhu W, Gong H, Han Y, Zhang M. van Duin ACT. Development of a reactive force field for simulations on the catalytic conversion of C/H/O molecules on Cu-metal and Cu-oxide surfaces and application to Cu/CuO-based chemical looping. J Phys Chem C 2020;124:12512–20.
[22] Senftle TP, Hong S, Islam MM, Kylasa SB, Zheng Y, Shin YK, et al. The ReaxFF reactive force-field: development, applications and future directions. npj Comput Mater 2016;2:1–14.
[23] Senftle TP, van Duin ACT, Janik MJ. Determining in situ phases of a nanoparticle catalyst via grand canonical Monte Carlo simulations with the ReaxFF potential. Catal Commun 2014;52:72–7.
[24] Yan X, Duan C, Sun R, Ji X, Zhang Y, Chu H. Revealing the nitrogen migration mechanism during pyrolysis and steam gasification of biomass: a combined ReaxFF MD and DFT study. Fuel 2024;369:131739.
[25] Feng W, Zheng M, Bai J, Zhang X, Wu C, Guo Z, et al. Dynamic structure transformation of char precursors during co-pyrolysis of coal and HDPE by using ReaxFF MD simulation and experiments. Chem Eng J 2023;472:145100.
[26] Gao Y, Guo Y, Guan Y, Ma H. New insights into the carbon chain structure of alcohol on the combustion of diesel surrogates using ReaxFF molecular dynamics simulations. Chem Phys 2023;574:112035.
[27] Zhong Q, Zhang Y, Shabnam S, Mao Q, Xiao J, van Duin ACT, et al. ReaxFF MD simulations of petroleum coke CO_2 gasification examining the S/N removal mechanisms and CO/CO_2 reactivity. Fuel 2019;257:116051.
[28] Yao L, Zhang F, Song Z, Zhao X, Wang W, Mao Y, et al. ReaxFF MD simulation of microwave catalytic pyrolysis of polypropylene over Fe catalyst for hydrogen. Fuel 2023;340:127550.
[29] Guo S, Lu K, Zheng K, Yu X, Ren P, Yang Y, et al. Atomic-level insight into the carburization process of iron-based catalysts: a ReaxFF molecular dynamics study. J Catal 2024;438:115719.
[30] Fu J, Liu C, Li Y, Gong H. ReaxFF reactive molecular dynamics study on methanation reaction from syngas. J Phys Chem C 2023;127:8557–75.
[31] Loi QK, Searles DJ. Reaction dynamics of CO_2 hydrogenation on iron catalysts using ReaxFF molecular dynamics simulation. Langmuir 2024;40:18430–8.
[32] Yang Y, Zhou J, Yu Y. Understanding the oxidation mechanism of Fe(100) in supercritical CO_2: a ReaxFF molecular dynamics simulation. J CO_2 Util 2022;63:102119.
[33] Wang Y, Gao W, Li K, Zheng Y, Xie Z, Na W, et al. Strong evidence of the role of H_2O in affecting methanol selectivity from CO_2 hydrogenation over Cu-ZnO-ZrO_2. Chem 2020;6:419–30.
[34] Stangeland K, Li H, Yu Z. Thermodynamic analysis of chemical and phase equilibria in CO_2 hydrogenation to methanol, dimethyl ether, and higher alcohols. Ind Eng Chem Res 2018;57:4081–94.
[35] Nielsen ND, Jensen AD, Christensen JM. The roles of CO and CO_2 in high pressure methanol synthesis over Cu-based catalysts. J Catal 2021;393:324–34.
[36] Vu TTN, Desgagnés A, Iliuta MC. Efficient approaches to overcome challenges in material development for conventional and intensified CO_2 catalytic hydrogenation to CO, methanol, and DME. Appl Catal, A 2021;617:118119.
[37] Liu S, Zhao Q, Han X, Wei C, Liang H, Wang Y, et al. Proximity effect of Fe–Zn bimetallic catalysts on CO_2 hydrogenation performance, vol. 29. Transactions of Tianjin University; 2023. p. 293–303.
[38] Grabow LC, Mavrikakis M. Mechanism of methanol synthesis on Cu through CO_2 and CO hydrogenation. ACS Catal 2011;1:365–84.
[39] S P. Fast parallel algorithms for short-range molecular dynamics. J Comput Phys 1995;1:1–19.
[40] Aktulga HM, Fogarty JC, Pandit SA, Grama AY. Parallel reactive molecular dynamics: numerical methods and algorithmic techniques. Parallel Comput 2012;38:245–59.
[41] Wang J, Wang G. Dynamic evolution of methane oxidation on Pd-based catalysts: a reactive force field molecular dynamics study. J Phys Chem C 2022;126:14201–10.
[42] Chenoweth K, van Duin ACT, Goddard WA. ReaxFF reactive force field for molecular dynamics simulations of hydrocarbon oxidation. J Phys Chem 2008;112:1040–53.
[43] Nose S. A unified formulation of the constant temperature molecular dynamics methods. J Chem Phys 1984;81:511–9.
[44] Yu J, Dang Q, Wu T, Wu Y, Lei T, Qi F. Catalytic hydropyrolysis of lignin: insights into the effect of Ni catalyst and hydrogen using ReaxFF molecular dynamics simulation. J Anal Appl Pyrolysis 2023;175:106212.
[45] Mao Q, van Duin ACT, Luo KH. Investigation of methane oxidation by palladium-based catalyst via ReaxFF Molecular Dynamics simulation. Proc Combust Inst 2017;36:4339–46.
[46] Han Y, Ma T, Chen F, Li W, Zhang J. Supercritical water gasification of naphthalene over iron oxide catalyst: a ReaxFF molecular dynamics study. Int J Hydrogen Energy 2019;44:30486–98.
[47] Leonzio G, Zondervan E, Foscolo PU. Methanol production by CO_2 hydrogenation: analysis and simulation of reactor performance. Int J Hydrogen Energy 2019;44:7915–33.
[48] Döntgen M, Przybylski-Freund M, Kröger LC, Kopp WA, Ismail AE, Leonhard K. Automated discovery of reaction pathways, rate constants, and transition states using reactive molecular dynamics simulations. J Chem Theor Comput 2015;11:2517–24.
[49] Zeng J, Cao L, Chin C, Ren H, Zhang JZH, Zhu T. ReacNetGenerator: an automatic reaction network generator for reactive molecular dynamics simulations. Phys Chem Chem Phys 2020;22:683–91.
[50] Kim S, Kim J. The optimal carbon and hydrogen balance for methanol production from coke oven gas and Linz-Donawitz gas: process development and techno-economic analysis. Fuel 2020;266:117093.
[51] Din IU, Shaharun MS, Naeem A, Alotaibi MA, Alharthi AI, Nasir Q. CO_2 conversion to methanol over novel carbon nanofiber-based Cu/ZrO_2 catalysts—a kinetics study. Catalysts 2020;10:567.
[52] Yang Y, Evans J, Rodriguez JA, White MG, Liu P. Fundamental studies of methanol synthesis from CO_2 hydrogenation on Cu(111), Cu clusters, and Cu/ZnO(0001). Phys Chem Chem Phys 2010;12:9909.